Low Mass Human Mission to Mars
Blue Team - Mission Design Report

Louí Byrne, Kristoffer Seidel, Bora Günay, Benedikt Sosa, Hemanth Venkatesan, Johannes Götz
All authors are MSc students at KTH Royal Institute of Technology, Stockholm, Sweden
March 20, 2022

***Abstract*—This report details the design of a low mass human mission to mars given the objective of being the first humans to set foot on the red planet. Initial mission design specifications were attained from a literature study. Design tools such as analytical and numerical simulations were used to develop the specific mission that will be presented in this report. The following is a summary of the findings of this study and an overview of one suggested mission design for a Pythom Space mission.**

The optimal launch window for leaving earth orbit was found to be in October 2026, arriving on Mars in August 2027. This timeline offered the best compromise between being competitive in the race to Mars and having sufficient time to fund and prepare the mission. The option to postpone the mission until 2028 was considered as this initial schedule was deemed ambitious.

A long stay 1007 day mission was found to be the most feasible option given the technological limits of modern propulsive technologies restricting the option of a short stay mission. Of this 1007 days, 304 days would be spent in transit from Earth to Mars, and 336 days would be spent on the return leg. This gives 368 days in orbit around mars in an elliptical parking orbit, of which 23 days would be spent on the surface.

Keywords: Manned Mars Mission, Patched Conics, Trajectory, Spaceflight Simulation, Candor Chaos

A. Nomenclature

LEO - Low Earth Orbit
LMO - Low Mars Orbit
MAV - Mars Ascent Vehicle
MDV - Mars Descent Vehicle
SOI - Sphere of Influence
CMPO - Circular Mars Parking Orbit
EMPO - Elliptic Mars Parking Orbit
C.R.I.M.S.O.N - Crewed Return Interplanetary Mission for Surface Observation and New research

B. Symbols

$\vec{a}_1$ - acceleration of body 1
$\vec{a}_2$ - acceleration of body 2
$\vec{r}_1$ - Position vector of body 1
$\vec{r}_2$ - Position vector of body 2
$\vec{v}_1$ - Velocity of body 1
$\vec{v}_2$ - Velocity of body 2
$\vec{F}_1$ - Force acting on body 1
$\vec{F}_2$ - Force acting on body 2
a - Semi major axis
g_0 - Earth Gravity
h - Step size for Runge-Kutta-Algorithm
i - Inclination
m_f - Final Mass
m_p - Propellant Mass
m_0 - Initial Mass
m_1 - Mass of body 1
m_2 - Mass of body 2
$n_{engines}$ - Number of engines
t - Time
v_{esc} - Escape velocity
x_f - Ratio initial to final mass
y_n - Result n of Runge-Kutta-algorithm
E_k - Kinetic energy
E_p - Potential energy
F_{Thrust} - Engine thrust
G - Gravitational constant
I_{SP} - Specific Impulse
M_{Mars} - Mass of mars
R_{app} - Apogee radius
R_{per} - Perigee radius
T - Orbital period

I. Introduction

The goal of the C.R.I.M.S.O.N mission is to land the first humans on Mars with the constraint was minimising mission mass and hence maximising feasibility and economic viability. This mars mission is designed with the cooperation of 6 different teams for the Phytomspace company owned by Tom and Tina Sjorgen. The scope of mission design team is to cover all major aspects of mission scheduling, earth to mars trajectories, mars entry and landing, and return to earth. The initial design of the mission took inspiration from a NASA book that studies the options for a human mars mission, see [1]. This report details the mission that was designed around achieving the goal of putting the first humans on mars.

This report relies on a number of assumptions, mainly surrounding simplifications. Back of the envelop approximations were used throughout the report and so many numerical results are only valid as approximations. For the Mars ascent ΔV calculations, atmosphere drag is neglected because it is seen that it's effect is small enough to disregard. Also ΔV due to steering is neglected for the ascent and descent rocket equation calculations. For the two-body problem only the influence of Mars and the spacecraft is taken into account in order to reduce the calculation effort.

This structure of the report follows the design of mission phases, simulations, scheduling, orbits, mars descent and sensitivity studies.

A. Mission Phases and Schedule

The whole Crimson mission was divided into 4 main phases: preliminary launches, interplanetary transfer, Mars operations and interplanetary return transfer and re-entry. A Gantt Chart type mission schedule can be found in Appendix Fig.20.

1) **Preliminary Launches**
Preliminary launch phase comprised of 4 different launch set and the purpose was to carry the required tools, materials and expendables to LEO. In the first launch set, 4 Falcon Heavy launchers were used for the fuels and tanks. In the second and third launch sets, 2 Falcon 9 launchers were used for the transfer of expendables, habitat tools and materials and MDVs. All the other payload and crew will be transferred with launch set 4 and 7 Kang vehicle are used for this launch set. This phase starts on November 2024 and lasts until November 2026 [2],[3].

2) **Interplanetary Transfer**
Interplanetary Transfer phase included the transfer from LEO to elliptical Mars orbit. It would start in November 2026 and would continue until September 2027 [2].

3) **Mars Operations**
The third phase of the mission would be Mars operations. Mars operations phase comprised of duration in Mars parking orbit, Mars landing, Mars surface operations and Mars ascent. The transfer vehicle would revolve Mars in the parking orbit for 368 days. Mars landing, surface operations and Mars ascent could be held anytime in this duration, and they could be completed in a month. At the beginning of Mars landing MDVs would detach and brake to enter the circular orbit before descending to Mars' surface. This phase would start on September 2027 and would last until September 2028 [4].

4) **Interplanetary Return Transfer and Re-entry**
The ascent vehicle (crew MDV) would be launched from the Martian surface to transfer vehicle at the end of Mars operations phase; the transfer vehicle starts its trip to Earth with a Hohmann transfer, this phase would last until August 2029 and at the end of it the re-entry capsule would detach from the transfer vehicle and perform a skip re-entry into the Earth's atmosphere, that would be followed by parachute deployment and landing in the Pacific Ocean.

II. Methods

A. Trajectory comparison

There are generally two classes of high-thrust Hohmann transfer trajectories available to get to Mars, conjunction-class and opposition-class.

Conjunction-class trajectories as in Figure 1 utilise the orbital alignment of Earth and Mars and result in long duration missions of around 1000 days. A Hohmann transfer makes up the transfer ellipse. This class of trajectory minimises overall mission ΔV to between 4 - 9 km/s and allows for Mars stays of between 300 - 600 days. The radiation dose received during interplanetary flight is less in this case when compared to the opposition class trajectory as the spacecraft never comes closer to the sun than earth orbit.

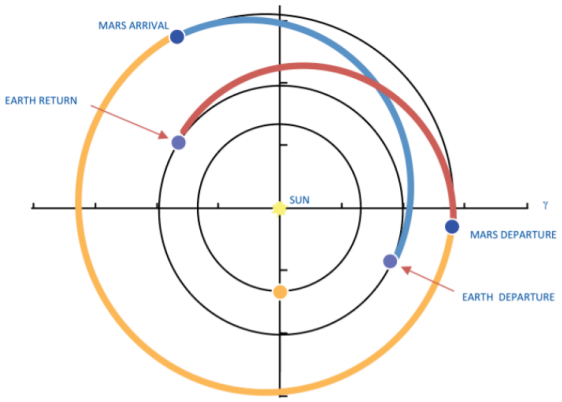

Fig. 1: Conjunction Class Trajectory [5]

Opposition-class trajectories as seen in Figure 2 offer short stays on Mars of around 30 - 90 days. The outbound Hohmann transfer from Earth to Mars is the same as in the conjunction class trajectory. The return leg utilises a higher-energy trajectory and requires the spacecraft to fly around the Sun before reaching Earth. The ΔV required for this class of trajectory is between 10 - 16 km/s and leads to total mission durations of 400-600 days. Conjunctions with Venus can offer the opportunity to perform a flyby and reduce ΔV but do introduce a closer approach to the sun, thus increasing radiation risk. The time spent in transit for opposition trajectories is greater than that for conjunction trajectories.

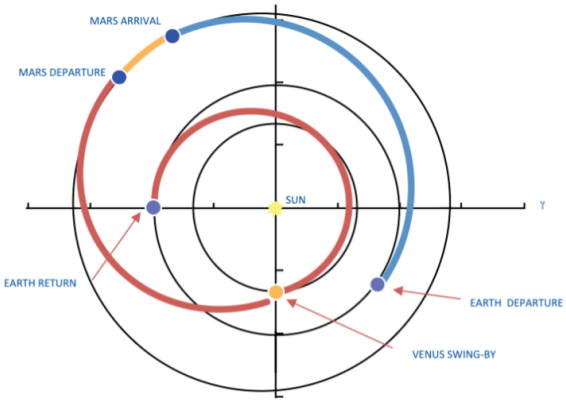

Fig. 2: Opposition Class Trajectory [5]

Considering these two options, the most suitable choice for our mission was found to be the one which minimises ΔV, and hence fuel mass. According to a comparison paper associated with NASA Langley research centre from 2014, there are major concerns with the capability of modern engines when

considering the ΔV required for opposition class trajectories [5]. As the goal of the mission was to put the first humans on Mars and the outbound leg of the trajectory was identical in both cases, it was found to be more feasible to achieve the lower ΔV requirements of a conjunction class mission, especially with a launch date in 2026. For this reason we have elected to choose a conjunction class mission.

B. NASA Trajectory Browser

The NASA Trajectory Browser is an open source tool that acts as a database. It stores pre-computed solar system transfer trajectories. It has been used to analyse launch windows from Earth to Mars and to choose the initial trajectory estimation for this mission.

Round trip, rendezvous trajectories were searched with a filter used to constrain the search to minimum ΔV options.

1) Limitations: The database provides solutions for direct transfers and simple fly-by-manoeuvres, but more complex manoeuvres were not handled. The trajectories are calculated using a Lambert solver and smaller celestial bodies are assumed to have zero mass. Other perturbations like solar radiation pressure are neglected.

2) Trajectory solver: The solution is obtained by determining the Keplerian transfer orbit connecting two celestial bodies considering the launch date and the transfer duration. Only the gravity of the sun is taken hereby into account, whereas all the other influences like gravity losses, the influence of other planets like Venus, Jupiter, Saturn etc. or of trajectory correction manoeuvres are neglected. After setting a start and an arrival date, the space is discretized and the Lambert equation will be solved. The round-trip-trajectories are calculated separately, thus we obtain a trajectory from Earth to Mars and one from Mars to Earth. The trade-off between the propulsion demand and the mission duration were also plotted and a compromise can be seen in Figure 3

C. Launch Windows

Figure 3 shows the launch windows from 2022 to 2028 with both short and long stay options. It shows that all short stay options exceed 10 km/s ΔV whereas long stay options are available at around 5 km/s.The 2026 launch window was considered to be the most ideal trade off between being the first to set foot on Mars and having enough time to prepare for and generate the financial backing for the mission. This launch window was deemed ambitious, as preparations would need to start now in order to have a fully designed mission and to launch to LEO in November 2024, less than 3 years from now. The launch windows in Q4 of 2028 offers an extra 2 years for preparations while maintaining very similar ΔV and mission duration requirements. The similarity between the launch conditions allow for a number of options regarding logistic alterations. The launch and assembly of components in LEO can be delayed by up to 2 years, or if the transfer ship has already been assembled, the interplanetary transfer burn can be postponed until Q4 2028. The 2028 option results in a very similar planetary alignment and thus mission schedule, resulting in this mission design report being valid for both the Q4 2026 and Q4 2028 launch windows with only small changes in design results.

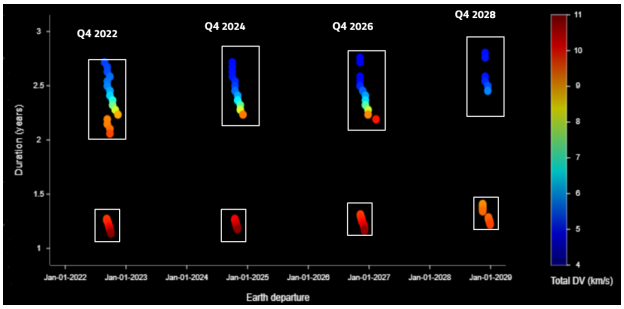

Fig. 3: NASA Trajectory Browser: ΔV Vs. Mission Duration [6]

1) Choosing a preliminary trajectory: The trajectory with the minimum ΔV requirements for the 2026 launch window was chosen as a preliminary trajectory. This choice is confirmed to be the most optimal for minimising ΔV as denoted by the 3.6 km/s dark blue area of the Q4 2026 launch window in the porkchop plots in Appendix Fig.21 and Fig.22. This information was used as a guide when building the MATLAB simulations and designing the initial mission schedule. The trajectory that was chosen from the NASA trajectory browser as the initial mission configuration has the properties in Table I.

TABLE I: Chosen Initial Trajectory from NASA Browser

Event	Time	ΔV (km/s)
Earth Departure	Nov 8 2026	3.36
Mars Arrival	Sept 08 2027	0.623
Mars Departure	Sept 10 2028	0.585
Earth Re-entry	Aug 12 2029	11.86 km/s re-enty

2) Alignment of planets: The alignment of mars and earth on the outbound transfer means that the distance between them varies between 1.3AU at launch and 2 AU at arrival as seen in Figure 4. The flight path of the transfer vehicle is denoted by the green path which follows a hohmann trajectory from earth to mars.

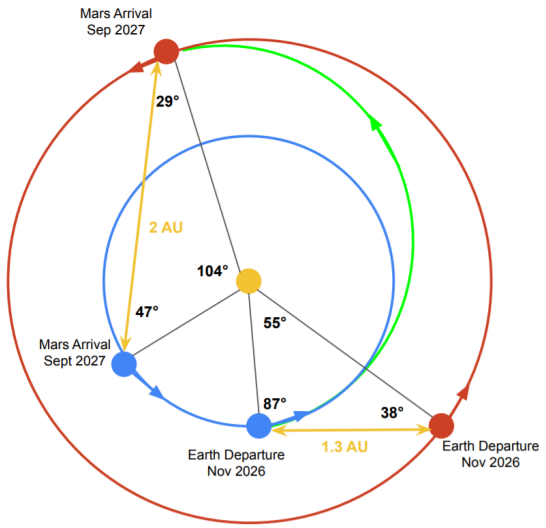

Fig. 4: Earth to Mars Transfer Trajectory

Figure 5 shows the return leg from mars to earth. it can be seen from the position of mars from arrival in Figure 4 to departure in Figure 5 that the duration of the mars stay is approx. one half mars year, and close to one full earth year. The most important feature of this alignment is that the direct line of sight, and hence communication, between earth and the transfer vehicle is never blocked by the sun during either of the outbound or return transfers.

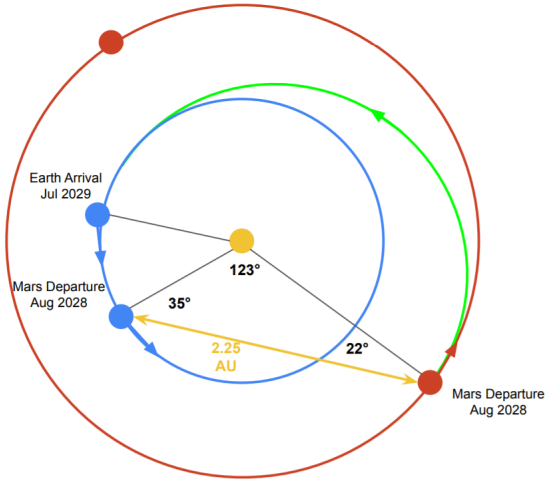

Fig. 5: Mars to Earth Transfer Trajectory

D. Trajectory Simulation

1) ΔV Estimation using the patched conics method: Typical interplanetary transfers is a complex feat to accomplish as the spacecraft is travelling between the spheres of influence of different planets, and to accomplish this transfer, must escape from the SOI of one planet to enter into the SOI of another. The patched conics method presents a simplification wherein the transfer ellipse between the departure and the target planet is patched together with hyperbolic escape and arrival trajectories. It is assumed that the spacecraft escapes from the departure planet with a finite velocity to execute a heliocentric transfer to the target planet to be captured around it in a hyperbolic arrival trajectory. It is still considered a two body problem, wherein the spacecraft in a planetary SOI travels in an unperturbed path around that planet and in a heliocentric orbit with the Sun as the primary while executing the transfer. Figure 6 depicts the path followed by a spacecraft while escaping from Earth's SOI.

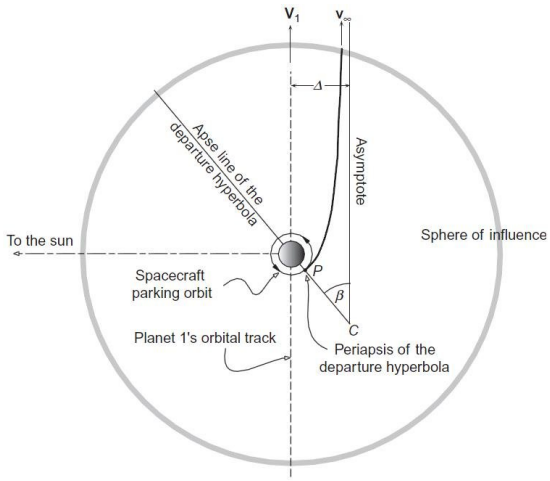

Fig. 6: Escape from Earth's SOI using a hyperbolic trajectory [7]

Although this method provided accurate results for our mission, it also demonstrated the sensitivity of the trajectory analysis to minute changes in the burnout speed provided while escaping from Earth. [7].

The effect of Earth's rotation was neglected during analysis.

2) Mid-course Manoeuvres: As previously mentioned, the patched conics method and the trajectory browser do not account for the perturbations in the path of the spacecraft due to the presence of other celestial bodies. During the interplanetary transfer, several mid-course corrections would have to be performed to account for the deviation from the actual trajectory due to the spacecraft escaping from the Earth's SOI with the wrong burnout speed; or the perturbations caused due to the gravitational influence of asteroids and other planets.

McElhoe in his paper describes a method to approximately calculate the required corrections for a transfer from Earth to Mars [8].

Table II lists all the mid-course manoeuvres required for the forward and return leg and the time intervals between them.

TABLE II: List of midcourse corrections, [8]

Earth-Mars		
Correction	Time (days)	ΔV_1 (fps)
First	73	92
Second	139	40
Third	150	60
Approach	0.43 hrs	22.7
Mars-Earth		
Correction	Time (days)	ΔV_1 (fps)
First	260	13.5
Second	472	34
Third	550	75
Approach	1.5 hrs	150
Total		245
Total		74.676 m/s

3) Δ V requirement for orbital inclination change: The Martian orbital plane is at an angle of 1.848° with respect to the ecliptic [9]. A good thumb rule while calculating the Δ V required for inclination change for an interplanetary transfer is to launch the spacecraft into a transfer orbit parallel to the ecliptic and making the inclination change mid-course when the true anomaly change remaining to intercept is 90° [10].

Figure 7 gives the optimal plane change point for the transfer between Mars and Earth. Eq.1 gives the ΔV required to effect such a change.

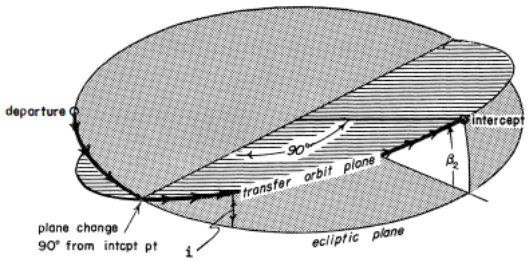

Fig. 7: Optimum plane change [10]

$$\Delta V = 2V \times sin\frac{i}{2} \tag{1}$$

E. Mars Parking Orbit

In choosing a parking orbit some constraints had to be set, namely that the descent could not take longer than the 8 hours for which the typical space suit could provide life support. Also that the orbital time of the parking orbit couldn't be too large, reason being the possibility to get back to the transfer vehicle in case of an off-nominal occurrence. There were also reasons of communication and energy requirements for the transfer vehicle which played a part. This time was set to be about 3 days. The closest point to Mars was limited to Mars atmospheric influence. Earths atmospheric density at 400km altitude is about equal to the Mars atmospheric density at 200 km [11]. This constraint was set to be able to assume no interference of the atmosphere on the parking orbit.

The choice was between a circular parking orbit and an elliptical one, both with different advantages and disadvantages. A circular orbit would have more frequent fly-bys of the landing site, necessary for landing the supply and crew MDVs. For an elliptical orbit the windows for descent become further apart, and when the MDVs would have to descend they would need a larger ΔV in order to do so. This parking orbit does require less ΔV to go into parking orbit, which would be very profitable, especially for the larger module which would not go to Mars surface. It is therefore worth doing an elliptical parking orbit when the two cases were compared in propellant used.

Doing an elliptical parking orbit would require some more operations to descend the MDVs. These included going from the elliptical orbit to a circular orbit at perigee, then waiting for the descent window and finally descending the MDV. It should be mentioned that when the supply MDV is in the circular orbit it leaves a cubesat to act as a connection between the astronauts and the transfer vehicle and lastly earth. This was important to establish reliable communication with earth.[4]

To define the exact attributes of the elliptical orbit these two principles were kept in mind. The closer the perigee and the further away the apogee the faster the velocity is at the perigee. As well, the closer the vehicles get to Mars the faster they would travel due to their potential energy converting into kinetic energy. The relative velocity of the transfer vehicle to Mars is 5580 m/s. It is therefore a question of how close should the vehicles get to Mars to have the least required ΔV to get into parking orbit.

Eq.2 to Eq.6 were used to calculate the semi-major axis, velocities, orbital periods, kinetic energy and potential energy respectively.

$$a = \frac{R_{app} + R_{per}}{2} \tag{2}$$

$$V(R) = \sqrt{\mu(\frac{2}{R} - \frac{1}{a})} \tag{3}$$

$$T(a) = 2\pi\sqrt{\frac{a^3}{\mu}} \tag{4}$$

$$E_K = \frac{mV^2}{2} \tag{5}$$

$$E_p = \int_0^h mg(h)\, dh \tag{6}$$

T in equation (4) is known as 72 hours. From that the semi major axis could be calculated. Using the semi-major axis, the velocity at perigee can be calculated using equation (3). Running this over many perigee radii, including the change in kinetic energy the following graph was acquired for perigee velocity, velocity due to potential energy and total ΔV needed to acquire the elliptical parking orbit. See Figure 15.

F. Simulation of the two-body problem

In order to validate the obtained models a numerical simulation is necessary. First of all, the two-body problem needs to be analysed in order to check the sensitivity of the Mars

orbits. The necessary data is extracted from NASA's Horizon System [12].

Newton's law of universal gravitation and Newton's second law provide the equations of motion to compute the orbits. [13] Newton's gravitational law in Eq.7 expresses the force $\vec{F}_1$ acting on body 1 dependent on the mass m_1 of body 1 in position $\vec{r}_1$ and the mass m_2 of body 2 in position $\vec{r}_2$ and also contains the gravitational constant G.

$$\vec{F}_1 = G\frac{m_1 m_2}{|\vec{r}_2 - \vec{r}_1|^3}(\vec{r}_2 - \vec{r}_1) \tag{7}$$

The acceleration $\vec{a}_1$ of body 1 can be calculated using Newton's second law as seen in Eq.8

$$\vec{a}_1 = \frac{\vec{F}_1}{m_1} \tag{8}$$

Considering an inertial system, Newton's law of universal gravitation can be written as a second order differential equation in Eq.9.

$$\ddot{\vec{r}}_1 = G\frac{m_2}{|\vec{r}_2 - \vec{r}_1|^3}(\vec{r}_2 - \vec{r}_1) \tag{9}$$

According to Newton's first law ("actio = reactio"), the same force $\vec{F}_2$ acts on body 2 in the opposite direction giving Eq.10.

$$\vec{F}_1 = -\vec{F}_2 \tag{10}$$

The acceleration of body 2 can be written similar to the acceleration of body 1 and gives Eq.11.

$$\ddot{\vec{r}}_2 = G\frac{m_1}{|\vec{r}_1 - \vec{r}_2|^3}(\vec{r}_1 - \vec{r}_2) \tag{11}$$

In order to solve this problem, the second order differential equation was transformed into a system of first order differential equations as follows in Eq.12

$$\begin{bmatrix} \vec{a}_1 \\ \vec{v}_1 \end{bmatrix} = \begin{bmatrix} \vec{v}_1 \\ G\frac{m_1}{|\vec{r}_1 - \vec{r}_2|^3}(\vec{r}_1 - \vec{r}_2) \end{bmatrix} \tag{12}$$

If the acceleration of body 2 is also taken into account, the system of differential equation is given by Eq.13.

$$\begin{bmatrix} \vec{a}_1 \\ \vec{v}_1 \\ \vec{a}_2 \\ \vec{v}_2 \end{bmatrix} = \begin{bmatrix} \vec{v}_1 \\ G\frac{m_1}{|\vec{r}_1 - \vec{r}_2|^3}(\vec{r}_1 - \vec{r}_2) \\ \vec{v}_2 \\ G\frac{m_2}{|\vec{r}_2 - \vec{r}_1|^3}(\vec{r}_2 - \vec{r}_1) \end{bmatrix} \tag{13}$$

This system was solved numerically using a fourth-order Runge-Kutta algorithm [14] denoted by Eq.14 - Eq.18

$$y_{n+1} = y_n + \frac{1}{6}h(k_1 + 2k_2 + 2k_3 + k_4) \tag{14}$$

$$k_1 = f(t_n, y_n) \tag{15}$$

$$k_2 = f(t_n + \frac{h}{2}, y_n + \frac{h}{2}k_1) \tag{16}$$

$$k_3 = f(t_n + \frac{h}{2}, y_n + \frac{h}{2}k_2) \tag{17}$$

$$k_4 = f(t_n + h, y_n + hk_3) \tag{18}$$

G. Mars Descent Simulation

In order to verify Mars descent calculations, a Matlab simulation program was written. The Descent phase was divided into 5 different stages: initial breaking, free fall (it could be set as throttled descent), throttled descent, parachute fall and powered descent.

Simulation program solved the same series of differential equations for all stages, however inputs and some effects (like air drag) were added, removed or changed according to the stages.

The equations of motion in the framework of the co-rotating spacecraft were at the top of these equations[15], Eq.19 and Eq. 20.

$$\frac{\mathrm{dv}}{\mathrm{dt}} = \frac{T}{m} - \frac{D}{m} - g\sin\gamma \tag{19}$$

$$\frac{\mathrm{d}\gamma}{\mathrm{dt}} = -\frac{1}{v}\left(g - \frac{v^2}{R_e + h}\right)\cos\gamma \tag{20}$$

Altitude and ground distances in the local vertical-local horizontal frame (LVLH) were the other equations, Eq.21 and Eq. 22, that were solved in this program.

$$\frac{\mathrm{dx}}{\mathrm{dt}} = (\frac{R_e}{R_e + h})v\cos\gamma \tag{21}$$

$$\frac{\mathrm{dh}}{\mathrm{dt}} = v\sin\gamma \tag{22}$$

H. Earth Reentry

Since the reentry speed in this mission was similar to the reentry speed of the Apollo missions, the same reentry procedure and angle are chosen. The reentry speed of 11,86 km/s leads to a high energy and heat input to the hull, so the spacecraft needs to be decelerated gradually. Therefore, a reentry angle $\gamma_e = 6.5°$ is chosen, whereas the window is about 2° wide. If the angle were too steep, the g-forces would increase tremendously, a too shallow angle would lead to inaccurate landing and would increase the risk of being bounced back into space. Like the Apollo missions, a double-tip is performed. The first tip would be flown forwards, so the lift vector bounces the spacecraft back into space, where it rotates and dives into the atmosphere again, but with a lift vector downwards in order to reach the landing spot more precisely. The g-force is about 6g, which can be handled by trained astronauts. During the final ballistic reentry, communication blackout lasts for 6 minutes due to intense vibrations and heat build up, the control system must be fully autonomous here with a manual control override in the event that the computer fails. Back in atmosphere, parachutes would be deployed to brake the free fall and to land the capsule safely. [13]

I. Propellant calculations

Based on the mission schedule and the different phases the amount of propellant in order to fulfil every requirement was calculated within a Matlab program. It took into account the changing mass after each burn and included course correction margins regarding ΔV which are explained in II-D2. The algorithm performed iterations to reach the required fuel mass as shown in Figure 8. Since the propellant mass is not known at the beginning of the mission, the algorithm is given the dry mass of each spacecraft as input and starts the first iteration with an estimate of the propellant mass for the respective mission phases.

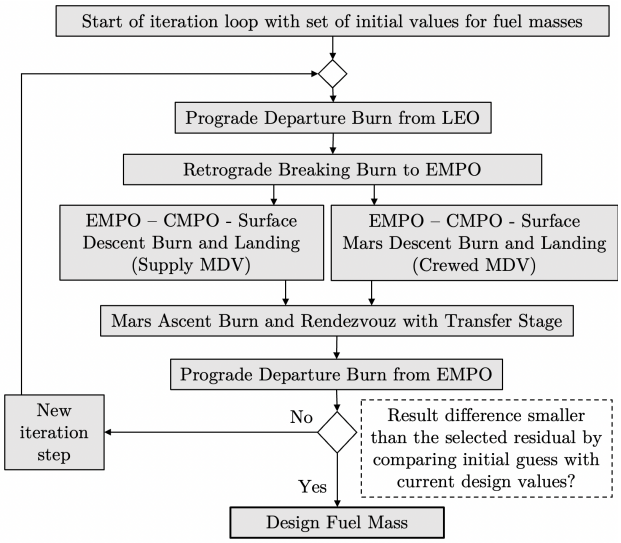

Fig. 8: Flowchart of iteration algorithm for estimation of propellant mass based on ΔV calculations

Using Tsiolkovsky's equation [16] the resulting propellant mass in order to achieve the required amount is given by Eq.23

$$m_p = m_0 \cdot (1 - exp(\frac{-\Delta V}{I_{SP} \times g_0})) \tag{23}$$

Whereby the initial mass consists of the propellant mass and the empty mass of the spacecraft.

$$m_0 = m_p + m_f \tag{24}$$

1) MDV Propellant masses: To calculate the needed propellant for the crewed MDV vehicle and the supply MDV the rocket equation was used. Since the structural and payload mass and the vehicles' mass was known the needed propellant could be calculated using equation (23) for the different phases in reversed order. Using the final mass of the crew MDV as: 570+330 = 900kg.[4] As the crewed vehicle needs 5000kg propellant the mass is distributed between the crew MDV and the supply MDV so that the masses would be distributed equally. Distributing the mass the effective payload mass becomes 3702 kg for both the descent and ascent vehicle (since the propellant for ascent was seen as payload). It should be clear that these are approximations, it is likely that more mass is needed to account for increasing structural mass when adding propellant and other effects which are not included in this approximation.

J. Descent Burn Window

Since the mission is to land in Candor Chaos a breaking maneuver must be performed and the thrust must be applied in a proper section of the orbit, see Fig. 9. Otherwise it would be required to wait one period of parking orbit. The proper orbit section and corresponding section time can be calculated. If we consider the Candor chaos, it has 810 kilometers length. For any point in the orbit, landing trajectory would be same so it is needed to use orbit altitude to calculate orbital section length. It only depends one these two parameters.

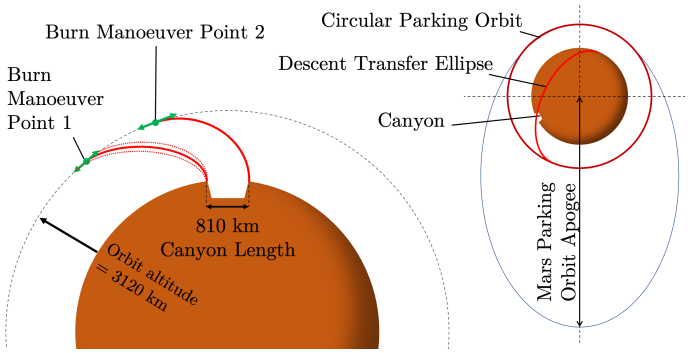

Fig. 9: Landing Site and Orbital Section, not to scale

This orbital section length can be calculated by using Eq.25.

$$L_{orbit} = \frac{(R_M + h_o rbit)}{R_M} \tag{25}$$

Then we can calculate the time interval that landing on Candor Chaos is possible, by dividing orbital section to orbital velocity giving Eq.26

$$\Delta T = \frac{810(R_M + h_{orbit})^{(3/2)}}{R_M \sqrt{\mu}} \tag{26}$$

In addition, to do further analysis beyond the assumptions of the patched conics method, firing time sensitivity was also looked at. The central goal of the mission is the manned landing in Canyon Candor Chaos. In order to achieve this goal, the time required for a thrust manoeuvre to enter a descent was calculated. To get a feeling in case no further manoeuvres can be possible on the descent, due to a system failure for example, the required burn time of the braking manoeuvre was calculated with Eq.27.

$$\Delta t = \frac{m_0 \times I_{SP} \times g_0}{n_{engines} \times F_{Thrust}} \times (1 - exp(\frac{-\Delta V}{I_{SP} \times g_0})) \tag{27}$$

This was derived from the general rocket equation and takes into account the performance data of the Asterex engines. Assuming a simple Hohmann transfer ellipse for the descent to the Martian surface, one can estimate how long the maneuver will take via the change in velocity required with it. Results of this analysis can be found in III-G.

III. Results

A. Δ V requirement for the mission- Analytical method

As shall be discussed in Sec. III-D, the velocity increments were calculated based on the chosen parking orbit around Mars and a circular parking orbit with a height of 400 km around the Earth. These values are representative of an analytical method to find the velocity increments for the mission.

Table III lists all the Δ V to complete the mission, excluding mars operations.

TABLE III: ΔV requirements for the mission

Earth-Mars		
ΔV	Value (km/s)	Comments
First	3.5563	Escape from Earth
Second	0.708	Capture by Mars
Third	0.7704	Inclination change
Mars-Earth		
ΔV	Value (km/s)	Comments
First	2.0890	Escape from Mars
Second	1.5842	Capture by Earth
Third	0.7704	Inclination change

B. Mars Descent Simulation

Mars descent simulation was run for different values of different parameters. Table IV shows the inputs for one of the runs that have better results than other ones.

In Figure 10, 11 and 12, the results of the simulation are presented. They show velocity change, altitude, ground distance and mass change with respect to time.

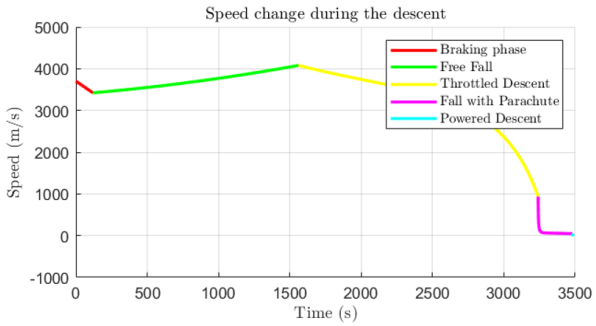

Fig. 10: MDV velocity change during Mars landing

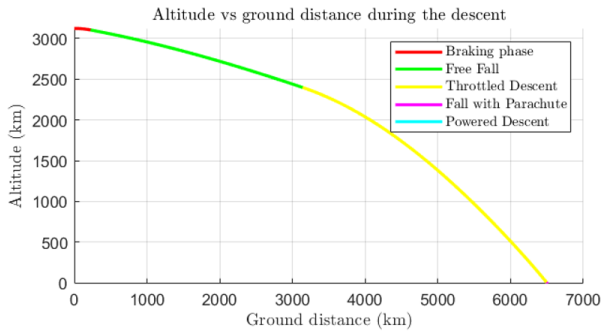

Fig. 11: Altitude vs ground graph for MDV

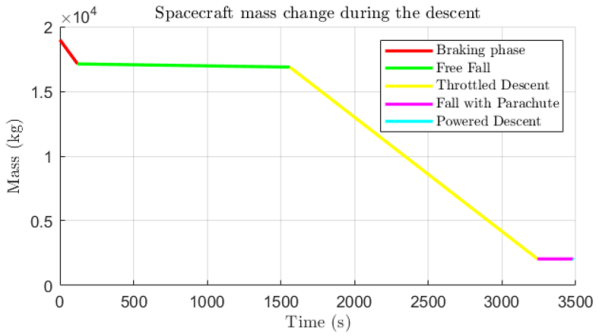

Fig. 12: Mass change of MDV

TABLE IV: Simulation Inputs

Phase	Duration (min)	Flight Angle (°)	Thrust (kN)
Retrograde Burn	2	5	45
Free Fall	24	10	0.5
Powered Descent	30	48	25.58
Parachutes	4	87	0
Final Burn	0.1	89.9	29

According to simulation results that are given in Figure 10, 11 and 12 when the vehicle is landed, final mass of the vehicle is 2035 kg while it's initial mass for the landing is 19000 kg. Landing takes 6500 km ground distance.

C. Fuel Mass Estimation

After running the patched conics method, including the simulation results from the descent and ascent simulation, the deviation from the initial estimate is determined and depending on the result, the resulting values are entered as a new estimate. This results in an iteration of the required fuel as can be seen in Figure 13 . After about 80 iterations the deviation is smaller than the set deviation limit of 1% and the mass is determined for each mission time.

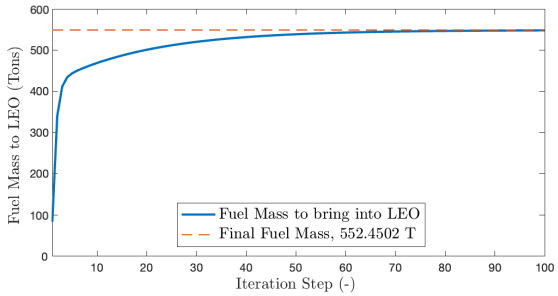

Fig. 13: Iteration of launch fuel mass in LEO

In Figure 14, the required propellant masses are listed per mission phase. The particularly high propellant mass at the beginning of the entire mission is especially significant as can be seen in 14. At departure from LEO with 448.86 tons, this was found to be considerably greater than, for example, the braking manoeuvre on arrival at Mars or the return journey. By using significantly heavier MDVs than in the preliminary design, the total mass at the beginning of the mission in

LEO increases considerably. The entire manned Mars mission, with the use of a transfer stage and multiple landing vehicles including return, would be extremely sensitive to subsequent course manoeuvres, so that each kilogram of payload and fuel for additional spacecraft would have a significant effect on the resulting total mass.

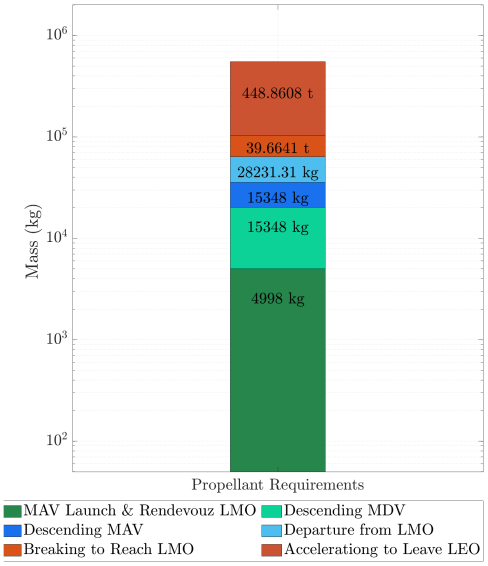

Fig. 14: Logarithmic distribution of required propellant mass

Additional information about propellant masses can be found in Tab. V.

TABLE V: Propellant Mass Details

Mission Phase	Maneuver	ΔV (km/s)	Propellant (kg)
Leaving Earth	Prograde Departure Burn from LEO	3.5563	448 860
Arriving Mars	Retrograde Breaking Burn to MPO (Elliptic)	0.801	39 664
Descending Supply MDV	Mars Descent Burn and Landing	4.74	15348
Descending Crewed MDV	Mars Descent Burn and Landing	4.74	15348
Ascent MAV & Rendevouz	Mars Ascent Burn and Rendevouz with Transfer Stage	5.436	4998
Leaving Mars	Prograde Departure Burn from LMO	0.585	28 231
	Total Amount	19.8583	552.45 t

In case of launch delays the possibility to return to the transfer vehicle would happen every 3 days. This waiting time could either be in the circular orbit if any issues were to arise once there, or on the surface of Mars if the problem were apparent before leaving the surface. If this were to occur twice then there would be enough life support supplies for the original mission duration and an additional 6 days.

For the astronauts safety, all life-necessary supplies were placed on the crew MDV. This would mean that if the supply MDV were to have an unsuccessful landing then it would not be a direct danger to the astronauts.

Table VI and Table VII show the propellant masses calculated for the MDVs.

TABLE VI: Masses needed for crew MDV

Propellant needed for crew MDV			
Phase	ΔV [m/s]	$m_{final}[kg]$	$m_{initial}[kg]$
CMPO-EMPO	918.2	900	1236
Surface-CMPO	4518	1236	5898
CMPO-Surface	3818	3702	13867
EMPO-CMPO	918.2	13867	19050

TABLE VII: Masses needed for supply MDV

Propellant needed for supply MDV			
Phase	ΔV	m_{final}	$m_{initial}$
CMPO-Surface	3818	3702	13867
EMPO-CMPO	918.2	13867	19050

D. Mars Parking Orbit

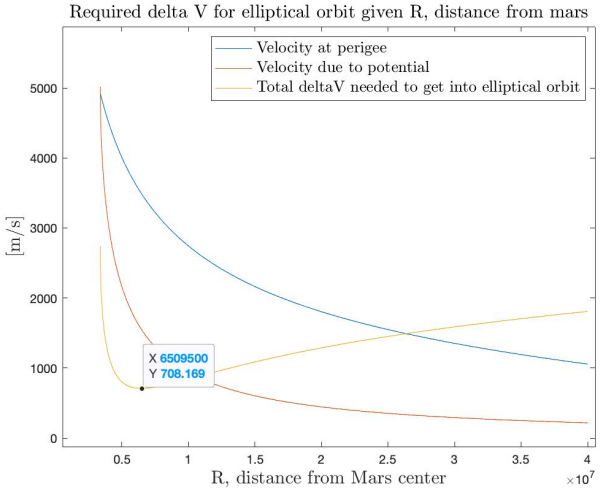

Fig. 15: Parking orbit attributes

Using Eq.2 the apogee radius was then calculated using the perigee value where the ΔV is minimum. See Figure 15.

This gives a possibility to launch back to the transfer vehicle every 72h which also was close to a multiple of the circular parking orbits period of 4.43h, this could be changed to match up perfectly very easily. This is a good thing for redundancy, in case an off-nominal scenario were to happen when the supply or crew MDV enters the circular orbit it can get back to the transfer vehicle after 3 days by adjusting the vehicles speed when the two orbits meet.

The final specifications of the parking orbits are the following: apogee is 77.028 million meters from Mars middle, perigee is at 6.5095 million meters. At perigee the velocity is 3485.9 m/s which gives 708m/s to get into elliptical orbit upon arrival.

E. Mars Entry, Descent, Landing and Ascent

1) Entry, Descent and Landing: In the correction burn the transfer vehicle aims its trajectory to go through a point 200km above Mars surface. As the vehicle passes this point it would execute a retrograde burn to achieve the desired elliptical orbit. Upon descent, the MDV would separate from the transfer

vehicle, it then does a retrograde burn to circularise the orbit and once at the descent window which occurs every 1.8 hours, the vehicle descends. Before descent the supply MDV leaves a cube-sat in circular orbit.

2) Ascent and Rendezvous: In order to dock with the spacecraft in the parking orbit, a rendezvous needs to be executed. Therefore, the MAV needs to reach the same elliptical parking orbit like the transfer vehicle. Since a crash needs to be avoided, the vehicles are phase-shifted. Using radial burns, it is possible to vary the distances between the spacecraft. As soon as the spacecrafts are within a few meters, the remaining distance can be covered by small steering burns. The rendezvous is performed in the apogee since the orbital speed is the lowest at this point and thus the steering and corrections are easier to perform. [13]

Fig. 16 shows the influence of a radial burn in direction of Mars surface on the duration to reach the apogee. The higher the ΔV is, the faster can the MAV reach the apogee and can catch up with the return vehicle. As soon as the MAV reaches the apogee of the elliptical parking orbit, another radial burn in the opposite direction needs to be performed to return to avoid a shifting of the orbit and to reach the elliptical parking orbit.

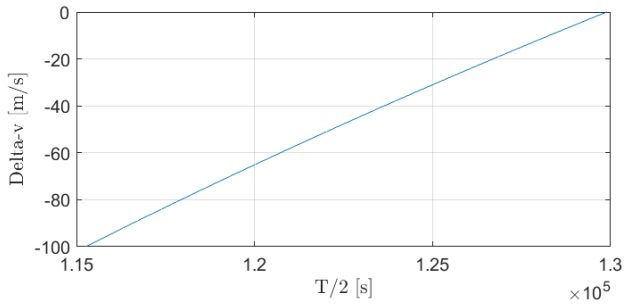

Fig. 16: Influence of ΔV for radial burns

F. Sensitivity of elliptical parking orbit

Using the two-body simulation, a sensitivity analysis of the elliptical parking orbit can be performed.

First of all, the influence of the perigee height on the apogee height is investigated, whereas the initial perigee speed is kept constant and is equal to the optimal perigee speed of 3485.9 m/s. Figure 17 shows the influence of the initial perigee height on the apogee height

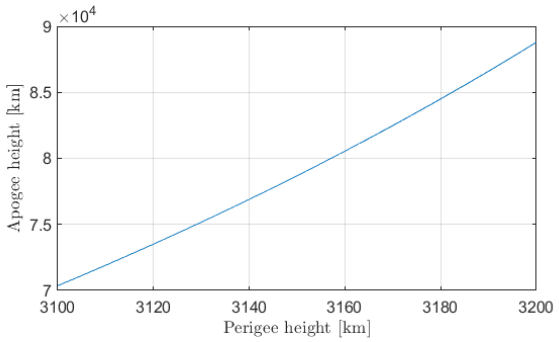

Fig. 17: Influence of the initial perigee height

The relation between the perigee height and the apogee height are nearly linear and a variation of the initial perigee height doesn't increase the danger of an uncontrolled escape from the gravity field.

It is also possible to consider a variation of the initial perigee speed and its influence on the apogee height, whereas the perigee height is kept constant at 3120 km. Figure 18 shows the results of the simulation.

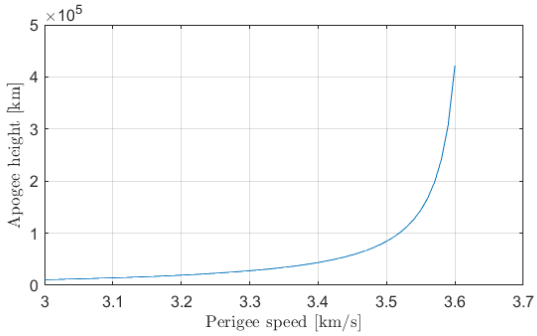

Fig. 18: Influence of the initial perigee speed

In comparison to the perigee height, the perigee speed has a much larger influence on the apogee height. The escape velocity of Mars can be calculated by Eq.28.

$$v_{esc} = \sqrt{\frac{2GM_{Mars}}{R_{per}}} = 3627 \ \frac{m}{s} \tag{28}$$

Since the optimal perigee speed of 3485.9 m/s is quite close to the escape velocity, the risk of an uncontrolled trajectory due to a increased initial speed is very high. Thus, the retrograde burn needs to be made very precisely in order to reach the elliptical parking orbit.

G. Off-Nominal Scenario

As presented above in section II, the deceleration sequence to land in the Chander Chaos was particularly studied. Landing in an exact area from such a high altitude can risk the whole mission, so the burn time window was calculated.

So for the 3120 km altitude this time interval corresponds to 446 seconds. If the supply MDV crashes the mission could be aborted, meaning that the crew MDV stays with the transfer vehicle. There is of course a possibility to go ahead with descending the crew MDV anyway but the mission would change significantly in that case given that mission critical supplies are on the supply MDV. In the case of a critical issue in circular LMO either upon descent or ascent the circular orbit of the MDVs and elliptical orbit of the transfer vehicle would meet up every three days. If an issue were to arise on the surface of Mars the case is the same. There would be a waiting period of at most 72.5 h depending on the position of the transfer vehicle.

Figure 19 shows the calculation of the burning time with a different number of engines. For the case of a descent ellipse as described above, the burn time for the thrust maneuver with only one main engine is about 652 seconds. If one departs from the assumption that a thrust maneuver takes place

in infinitesimal times, one would reduce the burn time by half and apply thrust before and after the maneuver point so that, on average, the desired trajectory is eventually achieved. Considering the time window of 446 seconds to land safely in the canyon, in case of a system failure there would be no time left to initiate a second ignition within the time window to complete the maneuver. For this reason, it is necessary that at least two main engines are installed on the MDVs so that a second, backup thrust sequence can be initiated and completed.

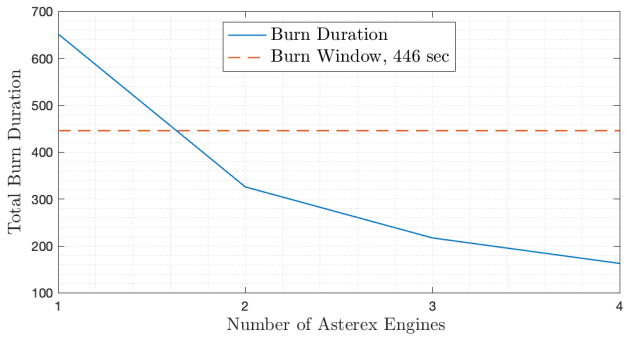

Fig. 19: Effect of engine number for resulting burn duration

IV. Discussion

A. Mars Descent Evaluation

The rocket equation and simulation, which are the two methods used for the Martian descent calculations, do not match with each other. While rocket equation gives payload capacity, according to simulation results these payload masses are not reachable. There are several possible reasons for this situation.

First one is the assumption that we use with rocket equation. When using the rocket equation, we assume that the velocity change resulting from burn will be gained instantly. However, this is not true, the velocity change is obtained during the total burn duration.

The other is that the velocity losses due to steering are neglected in the rocket equation calculations. However, these speed changes affect the simulation results. The effects of air drag was also neglected for rocket equation calculations since the effect of air drag is negligible effect like 50 m/s due to thin atmosphere of Mars.

B. Orbit Sensitivity

The retrograde burn which is used to reach the elliptical parking orbit, needs to be performed very precisely, whereas a deviation in the initial perigee height is rather less risky. On the other hand side, a deviation of the initial perigee speed leads to a great variation of the apogee height and increases the risk of leaving the influence of Mars rapidly.

V. Conclusion

Although the results obtained with the rocket equation are not achievable by simulation, these values were continued for other calculations. With the technological developments to be experienced in the future like parachutes with higher strength and higher speeds, more efficient and lighter rocket engines, landing optimisation algorithms, rocket equation results can be approached.

In order to calculate the orbits precisely other influences like solar wind, atmospheric drag or the gravitational influence of other planets need to be taken into account. Therefore a lot of additional simulations need to be done to guarantee a successful landing on Mars surface and a safe return to Earth.

When it comes to realising such a project it is clear that it will require an incredible amount of mass to get all the needed equipment into orbit, to Mars and back. This makes the project very complex not to mention logistically difficult and expensive to perform. Despite this, the results from this study show to a degree that this project is theoretically doable.

VI. Division of work

- **Louí Byrne** - Trajectory comparison, launch windows, initial trajectory choice.
- **Kristoffer Seidel** - Parking orbit, Mars descent, Mars ascent, MDVs.
- **Bora Günay** - Mission phases and schedule, descent launch application time delay, Mars descent and ascent.
- **Benedikt Sosa** - Multibody MATLAB simulations, rendezvous, orbit sensitivity analysis.
- **Hemanth Venkatesan**- Patched conics method, midcourse manoeuvres, analytical method for determining the velocity increments.
- **Johannes Götz** - Fuel estimation algorithm, patched conics method including mission phases, burn duration analysis.

References

[1] NASA Mars Architecture Steering Group. *Human Exploration of Mars*. NASA, July 2009.

[2] O. Malm T. Holmboe S. Weißenböck L. Wullschleger C. Segretin, K. Wen. Low mass mission to mars / blue team - transfer vehicle report. March 2022.

[3] L. Messmer S. Stenberg W. Josefsson Rudberg G. Dal Toso, J. Salminen. Low mass human mission to mars / blue team - logistics report. March 2022.

[4] N. Kusolphisarnsut M. Moore N. Moriya I. Taxis M. Dahlman, R. Franzè. Low mass mission to mars / blue team - mars operations report. March 2022.

[5] Bryan Mattfeld, Chel Stromgren, Hilary R. Shyface, David R. Komar, William M. Cirillo, and Kandyce E. Goodliff. Trades between opposition and conjunction class trajectories for early human missions to mars. *Space*, 2014.

[6] NASA. Trajectory browser, August 2021. URL `https://trajbrowser.arc.nasa.gov//`.

[7] Howard D. Curtis. *Orbital mechanics for engineering students*. Elsevier, 2020.

[8] Bruce A. McElhoe. An assessment of the navigation and course corrections for a manned flyby of mars and venus. *IEEE Transactions on Aerospace and Electronic Systems*, 1966.

[9] Dr. David R. Williams. Mars fact sheet.

[10] Jerry E. White Roger R. Bate, Donald D. Mueller. *Fundamentals of Astrodynamics*. Dover Publications, New York, 1971.
[11] A. Grasso Adrianos Golemis. Mars-x: Human exploration of mars from martian orbit. *Researchgate*, 2013.
[12] NASA. Horizons system.
[13] U. Walter. *Astronautics*. Springer, 2019.
[14] C. Karpfinger. *Höhere Mathematik in Rezepten*. Springer, 2017.
[15] Gunnar Tibert. *Fundamentals of Spaceflight Lecture Notes*. KTH, 2021.
[16] W. Steiner and M. Schagerl. *Raumflugmechanik*. Springer, 2004.
[17] Juan Luis Gonzalo. Easy porkchop.

APPENDIX

A. Mission Schedule

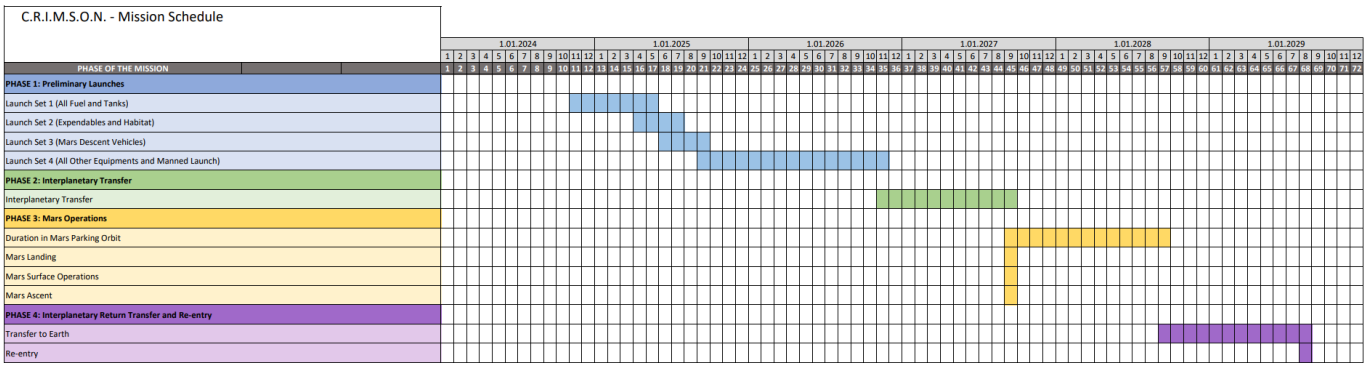

Fig. 20: Mission Schedule

B. Porkchop Plots 2026

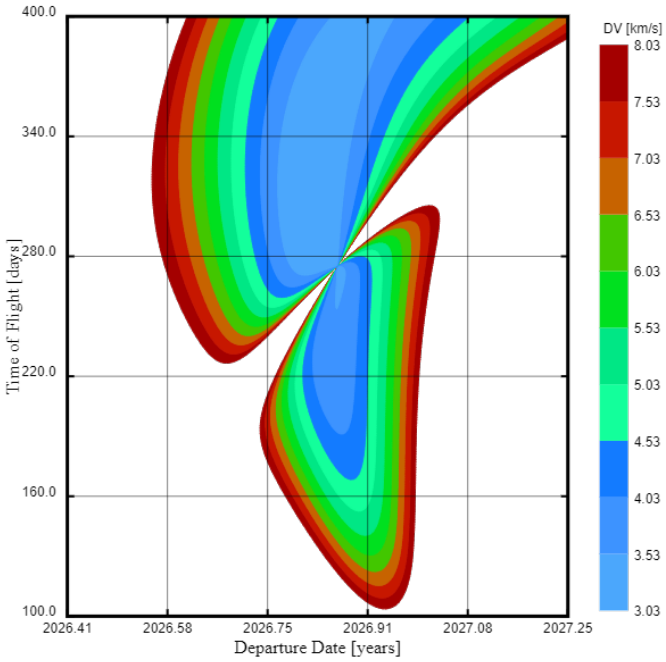

Fig. 21: Earth to Mars Departure ΔV Porkchop Plot [17]

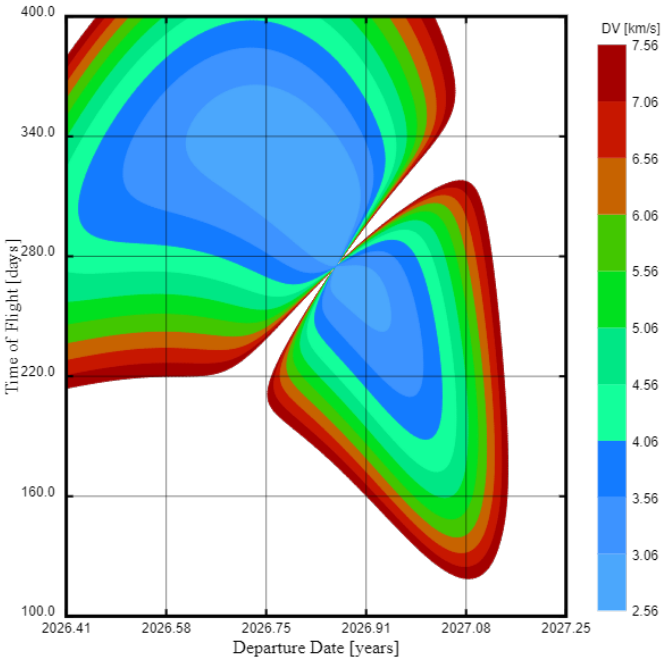

Fig. 22: Earth to Mars Arrival ΔV Porkchop Plot [17]